HYBRID MATERIAL BASED ON 5-(4-PYRIDYL)-10,15,20-TRIS(4-PHENOXYPHENYL)-PORPHYRIN AND GOLD COLLOID FOR CO_2 DETECTION

E. FAGADAR-COSMA[a*], A. LASCU[a], A. PALADE[a], I. CREANGA[a],
G. FAGADAR-COSMA[b], M. BIRDEANU[a,c]

[a]*Institute of Chemistry Timisoara of Romanian Academy, M. Viteazul Ave. 24, 300223-Timisoara, Romania,*
[b]*"Politehnica" University of Timisoara, Vasile Parvan Street 6, 300223-Timisoara, Romania,*
[c]*National Institute for Research and Development in Electrochemistry and Condensed Matter, 1 Plautius Andronescu Street, 300224 Timisoara, Romania*

The scientific community is aware of the importance of gold colloids and of their hybrids formed with biomimetic porphyrin for sensing and medical applications but also take into consideration the potential toxicity of gold nanoparticles. Starting from a bisfunctionalized porphyrin, 5-(4-pyridyl)-10,15,20-tris(4-phenoxyphenyl)-porphyrin, this study was focused to obtain a hybrid gold colloid–porphyrin and to use it for the detection of CO_2. Gold colloid having particles in a narrow range of diameters (15-18 nm) and proving long stability was obtained and complexed with the mixed substituted porphyrin in acid medium. The complex shows wide absorption in the whole UV-vis spectrum because the plasmon band was red-shifted with respect to the bare gold colloid nanoparticles and proved to be efficient for the CO_2 detection in wet environment. The Soret band increases in intensity as the concentration of CO_2 increases and the dependence is linear. TEM and AFM microscopy provided comparative data of the morphology and structure of the materials surfaces alone, as hybrid and after exposure to CO_2. The hybrid has double functionality because during its synthesis it can be considered as optical sensor for small amounts of gold and in the range of its stability is able to be an accurate gas sensor for CO_2.

1. Introduction

It is known that gold nanoparticles possess unusual properties. They can be easily put into evidence due to the presence of surface plasmon resonance (SPR) band and might increase the contrast of X-ray images, due to their capacity to absorb X-ray [1]. On the other hand, metallic nanoparticles alone, including gold, rise up issues regarding their toxicity, so that their presence in human body might be monitored. One of the actual proposed methods to solve the toxicity problem is to coat gold nanoparticles with biomimetic molecules, such as porphyrins, thus eliminating the direct contact with human living cells.

DNA decorated gold nanoparticles were used for biosensing [2] to detect extremely low concentrations of oligonucleotides and immunocomplexes and for the optical detection of enzymes [3, 4]. On the other hand, the surface of gold nanoparticles can be functionalized with receptors for hydrophobic anticancer drugs [5].

---

* Corresponding author: efagadar@yahoo.com

A hybrid system consisting of gold nanoparticles and manganese meso-tetra(pentafluorophenyl) porphyrin was use to modify fluorine tin oxide-coated glass electrodes and was successfully used for the sensing of cysteine [6].

Based on both the impressive metal coordination properties of porphyrins and on the presence of one pyridyl functional group in the porphyrin structure, that is able on one hand to improve coordination and on the other to be protonated and to increase polarizability and hydrophilicity, this this work was dedicated to development of novel colloids-dye hybrids [7] able to be used in detection of gases in order to monitor a safety environment. Starting from 5-(4-pyridyl)-10,15,20-tris(4-phenoxyphenyl)-porphyrin (PyTPOPP - Figure 1) and a gold colloid having particles of (15-18 nm) diameters a hybrid complex with wide absorption in the whole UV-vis spectrum was obtained.

The hybrid proved to provide double functionality because during its synthesis it can be considered as optical sensor for small amounts of gold and in the range of its stability is able to be an accurate gas sensor for CO_2.
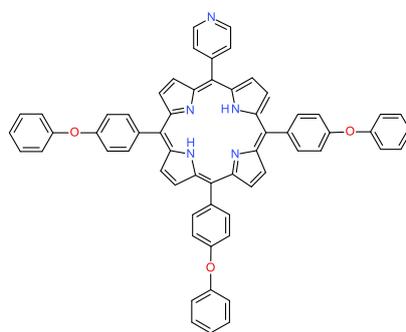
Fig. 1. Structure of 5-(4-pyridyl)-10,15,20-tris(4-phenoxyphenyl)-porphyrin

2. Experimental

2.1. Reagents

All reagents and solvents used in the experiments have been purchased from Sigma-Aldrich and Merck and were *purum analiticum* grade. Hydrogen tetrachloroaurate (III) trihydrate ($HAuCl_4 \cdot 3H_2O$) and trisodium citrate dehydrate, as reducing reagent, were used for preparing gold nanoparticles in a sustainable chemistry method [8].

The differentially functionalized porphyrin, *5-(4-pyridyl)-10,15,20-tris(4-phenoxyphenyl)-porphyrin,* was obtained by multicomponent Adler-Longo synthesis method, by using proper stoichiometry *(1/3)* of two different aldehydes, as previously published [9, 10].

2.2. Apparatus

UV-visible spectra were performed on a JASCO UV- V-650 spectrometer (Japan) using 1 cm pass cells. Atomic force microscopy (AFM) images were registered on Nanosurf®EasyScan 2 Advanced Research AFM (Switzerland). The surface imaging was done at room temperature with samples deposited from THF and water mixtures onto pure silica plates. AFM images were obtained in noncontact mode. TEM images were obtained on Titan G2 80-200 (FEI Company) instrument operating at 80 kV. Samples for TEM analysis were prepared on carbon-coated copper grids by deposition of diluted gold colloid solution.

3. Results and discussion

As shown in Fig. 2, the Soret main absorption band of the porphyrin is located at 419 nm and the four less intense Q bands are displayed at 515 nm, 551nm, 593nm and 650 nm decreasing in intensity from QIV to QI band. The gold plasmon has an absorption band at 525 nm.
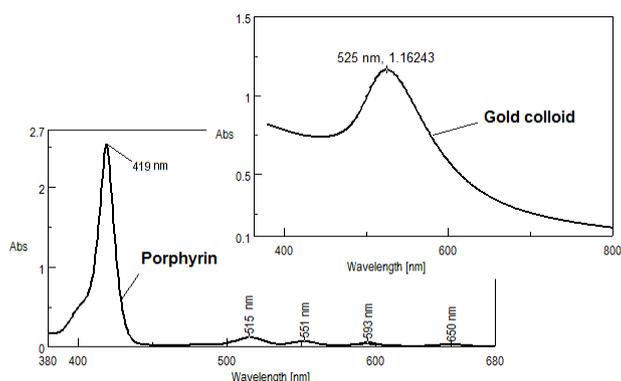
Fig. 2. UV-vis spectra of porphyrin (PyTPOPP) solution in THF and of gold colloid in water

The microscopic TEM characterization (Figure 3, C) of gold colloids nanoparticles put into evidence monodispersed spherical particles, with dimensions in a narrow range of 8-15 nm together with some triangular and ovoid shaped particles, of larger sizes, formed due to aggregation processes of gold in different directions. The AFM image, obtained by deposition on silica plates shows triangular aggregates (Figure 3, A), deposited in overlapped layers (Figure 3, B). The rugosity of the surface is 1.6 nm. The large-sizes triangular nanoparticles might be formed due to the trace presence of the reducing agent, which was reported to produce the association process [11].

A   B   C
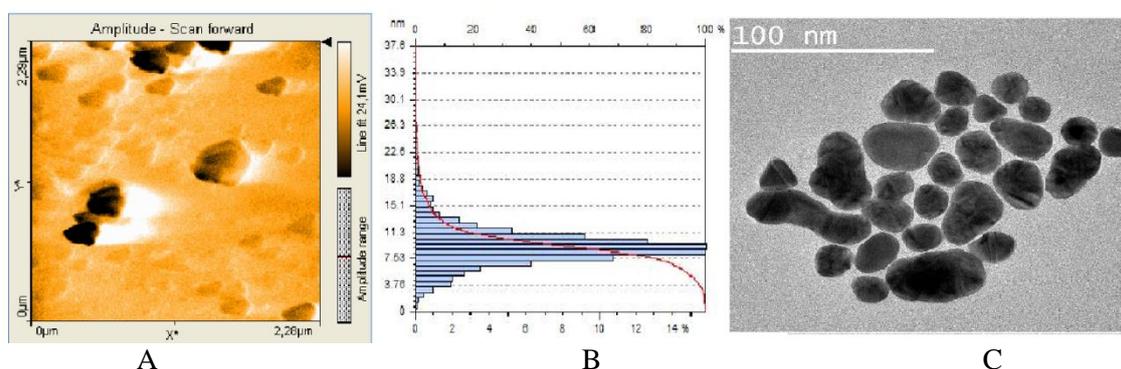
Fig. 3. AFM (A) and TEM (C) images of gold colloid in water.
AFM Distribution of the particles(B).

The hybrid porphyrin –gold colloid complex was obtained from 50 mL of 10^{-5} mole/L solution of 5-(4-pyridyl)-10,15,20-tris(4-phenoxyphenyl)-porphyrin in THF, in which small amounts, each of 2mL, of gold colloidal solution $(1 \times 10^{-4}$ mole/L) were slowly added under stirring.

Series of UV-Vis spectra (Figure 4) were recorded for each adding of gold colloid to the acidic solution of porphyrin (pH=4). With increasing amount of gold colloid, a continuous decrease in the intensity of the Soret bands was observed (Figure 4) accompanied by significant hyperchromic effect of all the four Q bands. Besides, a shift in the surface plasmon band to 531 nm in comparison with 525 nm band of bare gold colloid was observed, and this plasmonic band was continuously batochromic shifted reaching a plateau in a range of 531–549 nm. This red shift of surface plasmon absorption occurs because of a local increase in the refractive index around the gold particles when the complex with porphyrin is generated. Finally, the surface plasmon bands enmeshed the Q bands and their intensity is 20 times increased. The generation of this hybrid complex between gold and porphyrin is also certified by the clearly defined isosbestic point at 428

nm in the UV-vis spectrum. A change in color to violet-blue can be also noticed, that is not the result of usual combinations of green and red colors (Figure 5).
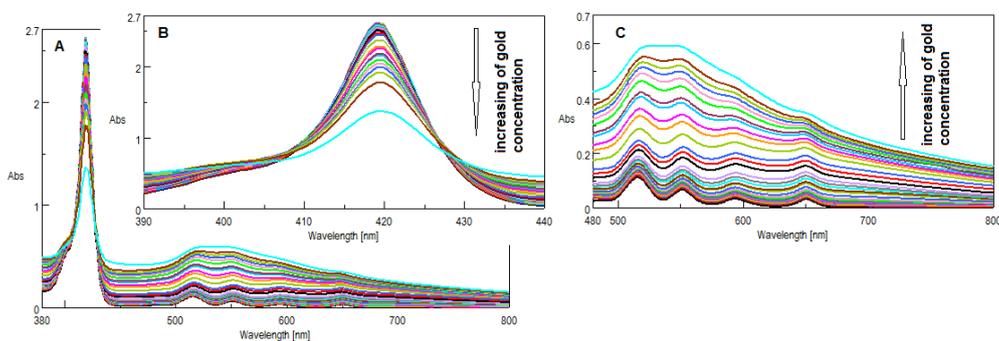
Fig. 4. UV-vis spectra of the hybrid formation(A); detail of Soret decrease in intensity by increasing gold concentration (B); detail of surface plasmon band increase by increasing gold concentration (C).

The dependence between the absorption intensity of the Soret band and the gold colloid concentration is linear, characterized by a good correlation coefficient of 0.983, meaning that the studied porphyrin is sensitive to gold detection in the range of low concentrations (Figure 5).
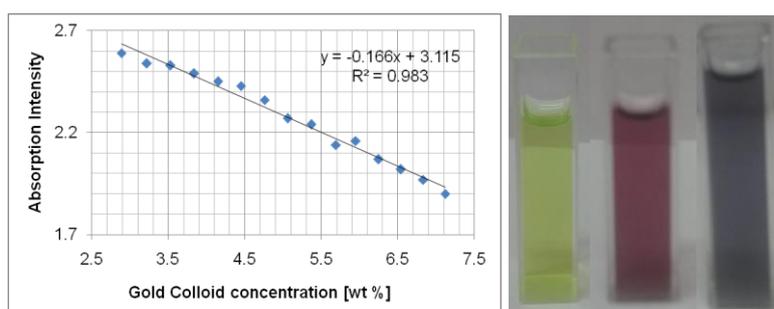
Fig. 5. The dependence between the absorption intensity of the Soret band and the gold colloid concentration. Changing in color from green porphyrin solution, red gold colloid to final violet-blue hybrid gold–porphyrin.

The AFM images of the hybrid gold colloid-porphyrin show a continuous covered surface with triangular shaped aggregates of uniform sizes, that is a common feature in porphyrin hybrid nanomaterials [12]. The rugosity of the material is decreased in comparison with gold surface from 1.6 nm to 0.41nm.
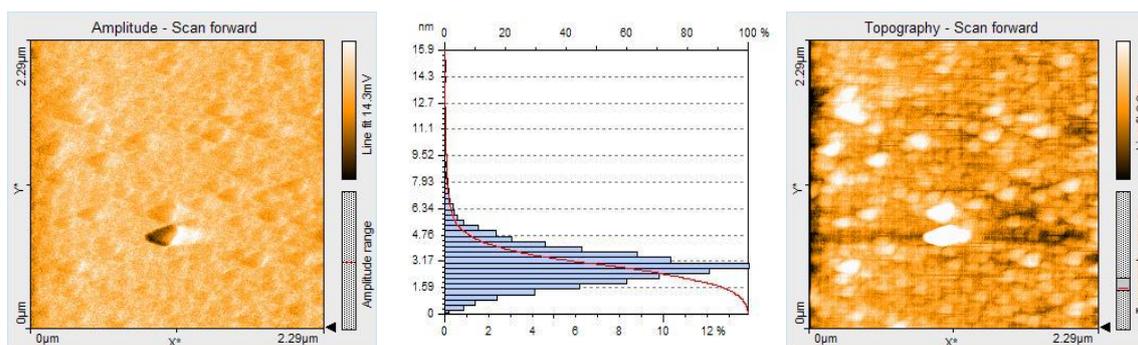
Fig. 6. AFM images, distribution and topography of hybrid gold colloid-porphyrin.

Because in our previous studies the same porphyrin-base linked in a PVP-polymer hybrid gave promising results to CO_2 detection [13], the actual gold-porphyrin hybrid was also exposed to CO_2 in wet environment. The experiment was monitored by UV-vis spectroscopy (Figure 7). For measuring the CO_2 influence, the CO_2 stream gas (1 mL min^{-1}) was bubbled into the gold-porphyrn complex solution (50 mL) under vigorous stirring.
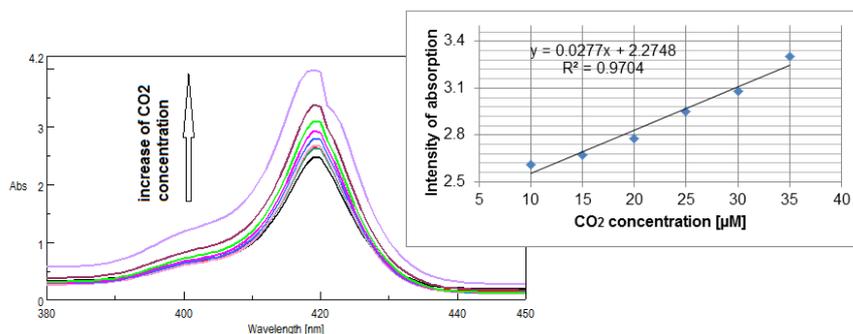
Fig. 7. UV-vis spectra of the hybrid exposed to CO_2 and the linear dependence between the Soret band intensity of absorption and the CO_2 concentration

Samples were measured by UV-vis spectroscopy each 5 minutes. In a very low range of concentration (10-35 μM), the dependence was linear, meaning that our purpose to realize a sensor able to detect trace amounts of CO_2 to be used in space habitacle is realized. Taken into consideration that 13 μM represents the normal concentration of CO_2 in air, our sensor can detect any abnormal increase, before rhythm acceleration or headaches to be provoked to the staff working on space orbital stations [14].

The 2D and 3D AFM images, after the hybrid was treated with CO_2, show a continuous morphology of the surface with few large sizes triangular aggregates of almost 300 nm, proving a rearrangement of the surface morphology (Figure 8).
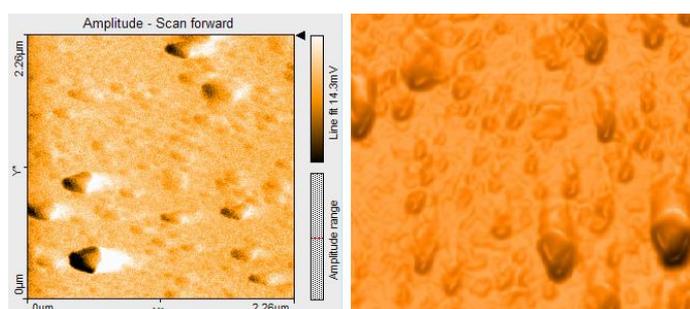
Fig. 8. 2D and 3D AFM images of gold colloid-porphyrin hybrid after CO_2 exposure.

4. Conclusions

This study was focused to obtain and characterize a hybrid gold colloid–porphyrin, based on 5-(4-pyridyl)-10,15,20-tris(4-phenoxyphenyl)-porphyrin . The changes produced by CO_2 on the gold colloid-porphyrin hybrid were investigated using UV-visible spectroscopy. The Soret band intensity increased continuously with increasing CO_2 concentration. As already reported by our team [13] in case of another hybrid of the same porphyrin linked in PVP polymer, the mechanism of CO_2 detection is not based on pH changes of the solution but on sorption phenomena which reorganize the surface morphology, as noticed by AFM. Taking into consideration that our sensor is able to detect very low range of concentrations (10-35μM) of CO2, and knowing that 13 μM

represents the normal concentration of CO_2 in air, our sensor can detect any abnormal increase, before producing damages to human life.

Acknowledgements

References

[1] Y. Kobayashi, R. Nagasu, T. Nakagawa, Y. Kubota, K. Gonda, N. Ohuchi, Nanocomposites, **2**, 83 (2015).

[2] E. Busseron, Y. Ruff, E. Moulin, N. Giuseppone, Nanoscale, **5**, 7098 (2013).

[3] S. Y. Park, A. K. R. Lytton-Jean, B. Lee, S. Weigand,G. C. Schatz, C. A. Mirkin, Nature, **451**, 553 (2008).

[4] D. Aili, R. Selegard, L. Baltzer, K. Enander, B. Liedberg, Small, **5**, 2445 (2009).

[5] C. Park, H. Youn, H. Kim, T. Noh, Y. H. Kook, E. T. Oh, H. J. Park, C. Kim, J. Mater. Chem., **19**, 2310 (2009).

[6] M. C. Gallo, B. M. Pires, K. C. F. Toledo, S. A. V. Jannuzzi, E. G. R. Arruda, A. L. B. Formiga, J. A. Bonacin, Synthetic Metals, **198**, 335 (2014).

[7] I. Creanga, G. Fagadar-Cosma, A. Palade, A. Lascu,C. Enache, M. Birdeanu, E. Fagadar-Cosma, Dig. J. Nanomater. Bios., **8**, 561 (2013).

[8] P. Muthukumar, S. Abraham John, Journal of Colloid and Interface Science, **421,** 78 (2014).

[9] E. Fagadar-Cosma, G. Fagadar-Cosma, M. Vasile, C. Enache, Curr. Org. Chem. **16**, 931 (2012).

[10] E. Fagadar-Cosma, Z. Dudás, M. Birdeanu, L. Almásy, Mat. Chem. Phys., **148**, 143 (2014).

[11] J. Lee, Y. H. Kim, H. Zhou, S. Hwang, K. Koh, W. D. Han, J. Lee, J. Mater. Chem., **21**, 13316 (2011).

[12] A. Lascu, A. Palade, G. Fagadar-Cosma, I. Creanga, C. Ianasi, I. Sebarchevici, M. Birdeanu, E. Fagadar-Cosma, Mat. Res. Bull., **74C**, 325 (2016).

[13] E. Fagadar-Cosma, E. Tarabukina, N. Zakharova, M. Birdeanu, A. Palade, I. Creanga, A. Lascu, G. Fagadar-Cosma, Polym. Int., **65**, 200 (2016).

[14] S. A. Rice, Rice and Associates, Inc., Grass Valley, CA, USA, Human Health Risk Assessment of CO_2: Survivors of Acute High-Level Exposure and Populations Sensitive to Prolonged Low-Level Exposure, *Third Annual Conference on Carbon Sequestration* **-** 2 May, Alexandria, Virginia, USA, 3-6 (2004).